



# FGF19 Analog as a Surgical Factor Mimetic That Contributes to Metabolic Effects Beyond Glucose Homeostasis

Alex M. DePaoli,<sup>1</sup> Mei Zhou,<sup>1</sup> Daniel D. Kaplan,<sup>1</sup> Steven C. Hunt,<sup>2,3</sup> Ted D. Adams,<sup>2,4</sup> R. Marc Learned,<sup>1</sup> Hui Tian,<sup>1</sup> and Lei Ling<sup>1</sup>

*Diabetes* 2019;68:1315–1328 | <https://doi.org/10.2337/db18-1305>

**Bariatric surgery has proven to be the most effective treatment for controlling hyperglycemia in severely obese patients with diabetes. We show that fibroblast growth factor 19 (FGF19), a gut hormone, is rapidly induced by bariatric surgery in rodents and humans. Administration of FGF19 achieves diabetes remission independent of weight loss in animal models of diabetes, supporting a role for FGF19 in the hormonal remodeling that restores metabolic function after the surgery. Through an unbiased, systematic screen in diabetic mice, we identified selective, safe, and effective FGF19 analogs. Unexpectedly, a lead FGF19 analog, NGM282, did not correct hyperglycemia in patients with type 2 diabetes. In contrast, administration of NGM282 resulted in a rapid, robust, and sustained reduction in liver fat content and an improvement in liver histology in patients with nonalcoholic steatohepatitis, faithfully replicating another key benefit of bariatric surgery. Our work identifies a strategy for replacing the surgery with an equally effective, but less invasive, treatment for nonalcoholic steatohepatitis.**

The growing incidence of obesity and type 2 diabetes globally is widely recognized as one of the most challenging contemporary threats to public health (1,2). Bariatric surgery, including Roux-en-Y gastric bypass (RYGB) and sleeve gastrectomy, is the most effective treatment for severe obesity and type 2 diabetes (3–5). Interestingly, the marked improvement in glucose homeostasis occurs early after the RYGB procedure before any appreciable weight loss (6). The underlying molecular mechanisms contributing

to these benefits remain an area of active investigation. There remains a significant need for pharmacological mimetics of these surgeries.

The resolution of type 2 diabetes after gastric bypass attests to the important role of the gastrointestinal tract in glucose homeostasis. Among the changes to gut physiology observed after gastric bypass surgery is altered enterohepatic circulation of bile acids, and significant increases in circulating total bile acids (TBAs) were observed in humans and rodent models (7–10). In this report, we show that levels of fibroblast growth factor 19 (FGF19), a gut hormone that plays a crucial role in controlling bile acid, carbohydrate, protein, and energy homeostasis (11), are elevated as early as 7 days postsurgery in humans. Using a large-scale, unbiased, *in vivo* screen, we have discovered safe and efficacious FGF19 analogs. One of these FGF19 analogs, NGM282, has recently demonstrated clinical efficacy in patients with chronic liver diseases, including nonalcoholic steatohepatitis (NASH) (12), primary sclerosing cholangitis (13), and primary biliary cholangitis (14). Furthermore, we present data from the first randomized, double-blind, placebo-controlled trial in our knowledge of an FGF19 analog in patients with type 2 diabetes.

## RESEARCH DESIGN AND METHODS

### NGM282 Clinical Trial in Patients With Type 2 Diabetes

In this multicenter, randomized, double-blind, placebo-controlled study in patients with type 2 diabetes inadequately controlled on metformin therapy, NGM282 was

<sup>1</sup>NGM Biopharmaceuticals, South San Francisco, CA

<sup>2</sup>Division of Cardiovascular Genetics, Department of Internal Medicine, University of Utah School of Medicine, Salt Lake City, UT

<sup>3</sup>Department of Genetic Medicine, Weill Cornell Medicine, Doha, Qatar

<sup>4</sup>Intermountain LiveWell Center, Intermountain Healthcare, Salt Lake City, UT

Corresponding author: Lei Ling, [lling@ngmbio.com](mailto:lling@ngmbio.com)

Received 11 December 2018 and accepted 2 March 2019

Clinical trial reg. no. NCT01943045, [clinicaltrials.gov](http://clinicaltrials.gov)

This article contains Supplementary Data online at <http://diabetes.diabetesjournals.org/lookup/suppl/doi:10.2337/db18-1305/-/DC1>.

© 2019 by the American Diabetes Association. Readers may use this article as long as the work is properly cited, the use is educational and not for profit, and the work is not altered. More information is available at <http://www.diabetesjournals.org/content/license>.

administered once daily through subcutaneous injection for 28 consecutive days. The trial protocol was approved by the ethics committees and institutional review boards (Dulwich, Australia, and Wellington, New Zealand) before study initiation. The study was conducted according to the provisions of the Declaration of Helsinki and in compliance with International Conference on Harmonisation Good Clinical Practice guidelines. All patients provided written informed consent before participation in the trial. The primary end point was absolute change in fasting plasma glucose from baseline to day 28. Secondary end points included the assessment of glycated hemoglobin (HbA<sub>1c</sub>), fructosamine, glucose tolerance, insulin resistance,  $\beta$ -cell function, body weight, safety, and tolerability. Exploratory end points included the assessment of serum levels of 7 $\alpha$ -hydroxy-4-cholesten-3-one (C4). Inclusion criteria were male and female patients with type 2 diabetes with inadequate glycemic control, 18–70 years of age with a stable body weight and BMI of 24–40 kg/m<sup>2</sup>, patients on metformin monotherapy with a fasting plasma glucose between 126 and 240 mg/dL, and patients on metformin combination therapy with a fasting plasma glucose between 126 and 210 mg/dL. Participants remained on their standard dose/regimen of antihyperglycemic medications (metformin alone or metformin plus other antidiabetic therapies) during the study. Exclusion criteria were type 1 diabetes, history of bariatric surgery, active acute coronary heart disease, clinically significant clinical laboratory abnormalities at screening, and acute electrocardiogram findings or significant variants at screening. A sample size of 16 completed participants per treatment group would provide 80% power to detect a difference in mean glucose changes from baseline of 41 mg/dL, assuming an SD of 40 mg/dL using a two-sided significance level of 0.05. To accommodate a dropout rate of up to 20% from randomization to study completion, a sample size of 20 randomized participants per treatment group (80 participants in total) was planned.

From November 2013 to July 2014, a total of 81 eligible patients were randomized in a 1:1:1:1 ratio to receive either NGM282 2 mg ( $n = 21$ ), NGM282 5 mg ( $n = 20$ ), NGM282 10 mg ( $n = 20$ ), or placebo ( $n = 20$ ). One participant in the NGM282 5-mg dose group was withdrawn from the study after randomization but before NGM282 dosing for taking prednisone and was excluded from the analysis. Participants self-administered the first dose under the supervision of site staff and returned to the study site on days 7, 14, 21, and 28 (end of treatment) for assessment. Participants returned to the study site on day 42 for a follow-up visit. Adverse events (AEs) were assessed using the Common Terminology Criteria for Adverse Events, version 4.03.

An oral glucose tolerance test (GGT) was conducted on days 1 and 28. Blood samples were collected pre-glucose load and at 30, 60, and 120 min post-glucose load. HOMA of insulin resistance (HOMA-IR) and HOMA of  $\beta$ -cell function (HOMA-bcf) were assessed from fasting glucose

and insulin levels on days 1 and 28 pre-glucose load. HbA<sub>1c</sub>, fructosamine, and body weight were measured on days 1 and 28 in all participants. Serum levels of C4 were only analyzed in the NGM282 2-mg and 5-mg groups.

### Patients for Gastric Bypass Surgery

From February 2010 through June 2011, 29 patients with severe obesity from a single bariatric surgical center (Rocky Mountain Associated Physicians, Salt Lake City, UT) seeking RYGB surgery were enrolled. All patients provided written informed consent to participate in the study. At baseline, 7 days, and 21 days postsurgery, a 250-mL standard liquid meal (1.5 calories/mL, 18% protein, 44% carbohydrate, and 38% fat) (Isosource; Novartis) was administered, and blood was drawn just before meal ingestion and 30 and 60 min after the meal.

### Animal Experiments

All animal studies were approved by the institutional animal care and use committee at NGM Biopharmaceuticals. Animals were housed in a pathogen-free animal facility at 22°C under a controlled 12-h light/dark cycle. All animals were kept on standard chow diet (Teklad 2918; Harlan Laboratories) and autoclaved water ad libitum unless otherwise specified. Male mice and rats were used. Animals were randomized into the treatment groups on the basis of body weight and blood glucose. All injections and tests were performed during the light cycle. C57BL/6J, *db/db*, TALLYHO, NONNZO, and *Fxr*-deficient mice were purchased from The Jackson Laboratory. Zucker *fa/fa* (ZF) rats were purchased from Envigo.

### Duodenal-jejunal Bypass Surgery in ZF Rats

RYGB causes rapid and dramatic weight loss in rodents to a much greater degree than in humans, which makes interpretation of early gene expression changes difficult. In contrast, duodenal-jejunal bypass (DJB), a surgical procedure that preserves the normal transit of nutrients through the stomach, does not result in substantial weight reduction, allowing us to focus on transcriptome change solely derived from the altered intestinal architecture. Therefore, we chose to use DJB instead of RYGB as the bariatric surgery procedure in the rodent studies. Surgical procedures were performed on 20-week-old ZF rats. DJBs were carried out as previously described (8,15). In brief, the abdominal cavity was exposed through a ventral midline incision. At 0.75–1 cm of the starting point of duodenum, a suture was tightly tied around the duodenum vertically, and a 0.4-cm horizontal incision was performed at this area; bowel continuity was interrupted at the level of the distal jejunum (10 cm from the ligament of Treitz). The distal limb was directly connected to the horizontal duodenum incision (duodenal-jejunal anastomosis), and the proximal limb carrying the biliopancreatic juices was reconnected downward to the alimentary limb at a distance of the same length of the entire bypassed duodenum and proximal jejunum from the duodenal-jejunal anastomosis.

For sham operations, rats underwent a surgical procedure similar to DJB, but all resections were reanastomosed to maintain the physiological circuit of food through the bowel. Rats were sacrificed 14 days after surgery, and intestines were harvested for RNA preparation and transcriptome profiling.

#### **db/db Mice**

For the unbiased, in vivo screen, 10- to 12-week-old *db/db* mice (BKS.Cg-*Dock7*<sup>m +/+</sup> *Lepr*<sup>db</sup>/J, #000642) were injected intravenously with  $3 \times 10^{11}$  vector genome of adeno-associated virus (AAV) carrying either FGF19 mutants or a control gene green fluorescent protein (GFP). During the 24-week study periods with continuous exposure to FGF19 mutant transgenes, *db/db* mice were subjected to glucose measurements at various time points and euthanized at the end of the studies for liver tumor quantification.

#### **Fxr-Deficient Mice**

*Fxr*-deficient mice [B6.129X1(FVB)-*Nr1h4*<sup>tm1Gonz</sup>/J, #007214] were fed a high-fat, high-fructose, high-cholesterol diet (HFFCD) (#D09100301i; Research Diets) to induce NASH. Treatment was initiated after 16 weeks of HFFCD feeding by injecting mice with  $3 \times 10^{11}$  vector genome AAV-FGF19, AAV-NGM282, or a control virus AAV-GFP through tail veins. HFFCD feeding was subsequently maintained for an additional 34 weeks, at which time mice were euthanized for histological and gene expression analysis.

#### **Statistics**

For studies in animals, results are expressed as the mean  $\pm$  SEM. One-way ANOVA followed by Dunnett posttest was used to compare data from multiple groups (GraphPad Prism). Two-way ANOVA followed by Sidak posttest was used to compare data when multiple groups and time points were involved (GraphPad Prism). When indicated, an unpaired Student *t* test was used to compare two treatment groups. Circulating FGF19 levels in patients before and after RYGB were evaluated by a paired two-tailed *t* test. For the NGM282 clinical trial in patients with type 2 diabetes, the change from baseline to day 28 was compared between treatment groups using ANCOVA, with treatment group as factor and baseline HbA<sub>1c</sub> and baseline end point value as covariates. Difference in least squares means, 95% CIs for the difference, and corresponding *P* values are presented. Within each treatment group, changes from baseline to day 28 were evaluated by a paired two-tailed *t* test. Statistical analyses for the clinical trials were carried out using SAS 9.4 software (SAS Institute, Cary, NC). Additional materials are provided in the Supplementary Data.

## **RESULTS**

### **FGF19 Is Induced by Bariatric Surgery in Rodents and Humans**

In an effort to identify potential gut-derived factors that could contribute to the beneficial effects of bariatric

surgery, we examined gene expression changes in various segments of the intestine before and after surgery using an established rodent model, DJB surgery in ZF rats (8) (Fig. 1A). DJB, a surgical procedure that preserves the normal transit of nutrients through the stomach, does not result in substantial weight reduction as seen with RYGB, allowing us to focus on transcriptome change solely derived from the altered intestinal architecture. Among the genes whose expression are differentially regulated by DJB versus sham procedures, FGF15 (the rodent ortholog of human FGF19) was one of the gut factors that showed the greatest increase in expression. Elevated levels of FGF15 mRNA were detected as early as 14 days postsurgery and likely resulted from the accelerated delivery of bile to the hind gut (Fig. 1B and C). Induction of *Nr1h4* (also known as farnesoid X receptor [FXR]) expression was also observed (Fig. 1B). Ingenuity pathway analysis of transcriptome profiling data revealed that several biological pathways, and transcriptional programs associated with cholesterol metabolism in particular, were enriched in the DJB group compared with the sham procedure group (Fig. 1D).

To determine whether these observations in animal models are recapitulated in humans, we measured FGF19 concentrations in serum samples from obese patients who had undergone RYGB surgery (Fig. 1E). Serum FGF19 concentrations increased significantly after RYGB in the majority of patients either under fasting conditions or after a standardized meal (Fig. 1F). The increase in serum FGF19 was observed as early as 7 days after surgery and persisted 21 days after surgery. Patient characteristics at baseline and postsurgery are shown in Supplementary Table 1. In summary, we observed significantly elevated levels of circulating FGF19 in rodents and humans as early as 7 days after bariatric surgery, supporting a role for FGF19 in the hormonal remodeling that restores metabolic function after the surgery.

### **Unbiased, Systematic, In Vivo Screen for the Identification of Efficacious, Nontumorigenic FGF19 Variants in *db/db* Mice**

Despite the demonstration of profound antidiabetic effects after administration of FGF19 in a variety of mouse models of diabetes (including monogenic *db/db* mice, polygenic TALLYHO and NONNZO mice, and  $\beta$ -cell-deficient mice) (Supplementary Fig. 1), potential safety concerns have hindered its development as a therapeutic for the treatment of type 2 diabetes. Although FGF19 has minimal mitogenic activity on fibroblasts and hepatocytes in vitro, ectopic expression of FGF19 in skeletal muscle of transgenic mice promotes hepatocyte proliferation, hepatocellular dysplasia, and neoplasia and, by 10–12 months of age, leads to the development of hepatocellular carcinomas (16). Multiple groups have endeavored to engineer safe and effective variants of FGFs, including FGF19 (17–20). Although the FGF19 mutants described in these reports

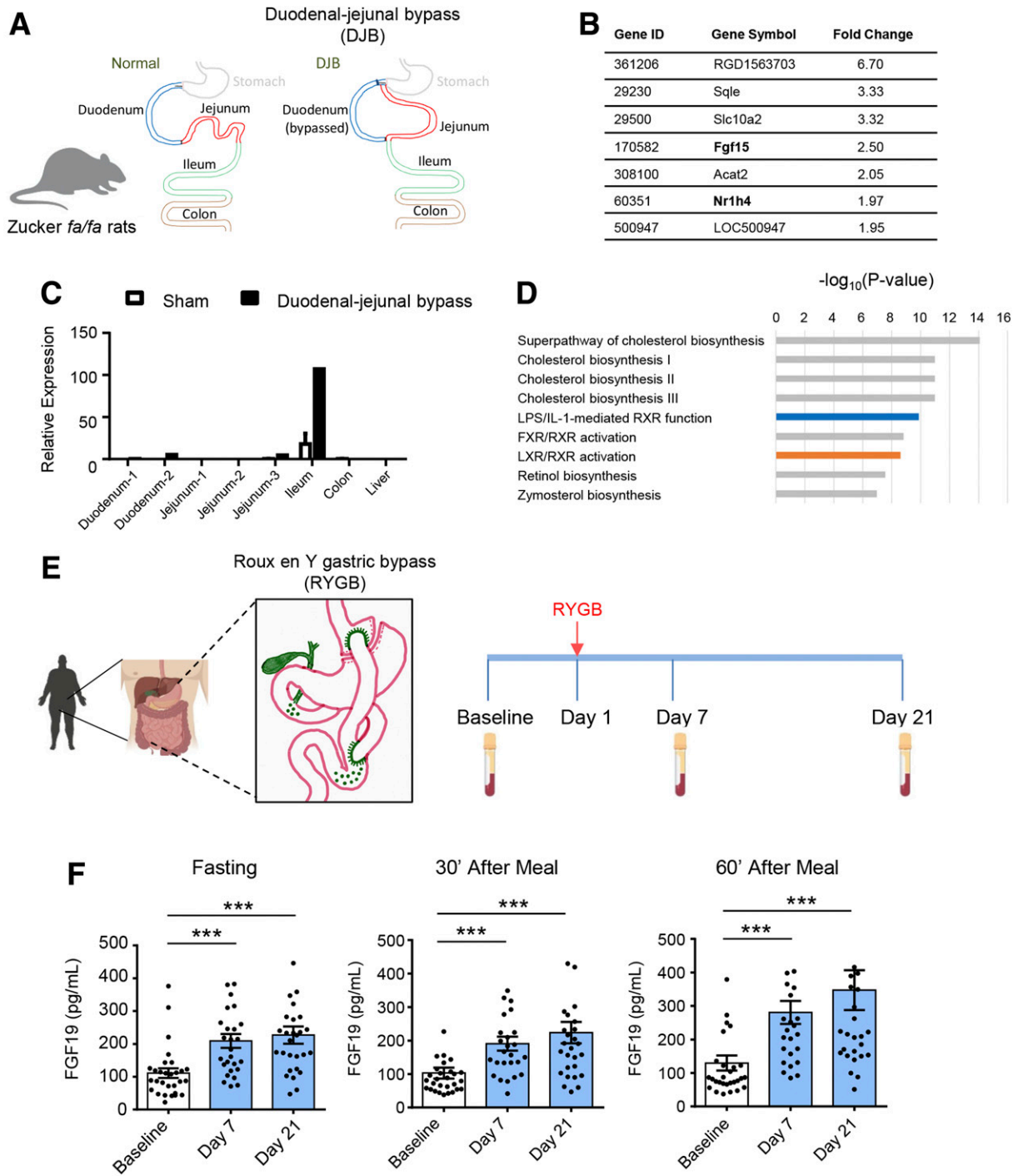


**Figure 1**— Levels of FGF15/FGF19 are elevated after bariatric surgery in rodents and humans. **A**: Schematic drawing of DJB surgery in ZF rats. The DJB procedure in rats resembles the RYGB procedure performed in humans. We hypothesized that in both DJB and RYGB, the bile, unmixed with food, is directly delivered to the distal jejunum and ileum where it induces FGF15/FGF19 expression in an FXR-dependent manner. Segments representative of the intestinal anatomy were collected in bypass and sham-operated animals. **B**: Top genes differentially induced by DJB surgery compared with sham procedure in ZF rats. Rats were sacrificed 14 days after surgery, and ilea were harvested for transcriptome profiling. *FGF15* and *Nr1h4* (also known as FXR) are shown in bold. **C**: Quantitative PCR analysis showing that mRNA levels of FGF15 were increased after DJB surgery in the ileum. Duodenum (in two segments), jejunum (in three segments), ileum, colon, and liver were harvested from ZF rats 14 days after sham or DJB procedures ( $n = 3$  biological replicates per group). **D**: Ingenuity pathway analysis of transcriptome profiling in ZF rats (DJB surgery vs. sham procedure). The top regulated canonical pathways are ranked by  $-\log_{10}(P \text{ value})$  with a threshold  $P = 0.05$ . Highest ranking categories are displayed along the x-axis in a decreasing order of significance. Orange bar, pathway with  $z \text{ score} > 0$  (upregulated pathway); blue bar, pathway with  $z \text{ score} < 0$  (downregulated pathway); gray bars, no activity pattern available. **E**: RYGB surgery in human patients. Serum samples were collected before surgery (baseline) and at 7 and 21 days postsurgery. **F**: Serum concentrations of FGF19 were increased after RYGB surgery in humans ( $n = 29$ ). Fasting as well as fed (30 or 60 min after meal [30' or 60']) FGF19 concentrations were determined. Data are mean  $\pm$  SEM. \*\*\* $P < 0.001$  by paired two-tailed  $t$  test. ID, identifier; LPS, lipopolysaccharide; LXR, liver X receptor; RXR, retinoid X receptor.



exerted modest glucose lowering in diet-induced obese mice, possibly secondary to the observed weight reduction in this model, they failed to improve the severe hyperglycemic condition when tested in *db/db* mice (Supplementary Fig. 2A–D). Moreover, significant safety concerns on these engineered FGF molecules, previously unrecognized from cell-based assays, were uncovered upon prolonged exposure of mice to these molecules (Supplementary Fig. 2E). Given the limitations of biochemical or cell-based assays for modeling complex, multisystem diseases, such as diabetes and cancer, we used an unbiased, systematic, in vivo screen to simultaneously assess glucose lowering and tumorigenicity of FGF19 mutants in *db/db* mice. During the course of this effort, we injected recombinant AAV carrying >150 FGF19 mutant transgenes intravenously into *db/db* mice for evaluation, monitoring blood glucose, body weight, and liver tumor formation over a 24-week study period. Detailed sequences of select mutants are included in Supplementary Tables 2–5 (and data not shown).

To establish a structure-activity relationship (SAR) and dissect FGF19 functional domains, we systematically changed predicted secondary structural elements in the FGF19 protein, including  $\beta$ -sheets, loops between  $\beta$ -sheets, and  $\alpha$ -helices (Supplementary Fig. 3A and B). Among these FGF19 mutants, mutation of the  $\beta$ 8– $\beta$ 9 loop region resulted in a marked reduction in the number of liver tumors compared with wild-type FGF19 without compromising the antidiabetic efficacy (Fig. 2A and B). This FGF19 variant also did not promote the increase in liver weight associated with prolonged exposure to wild-type FGF19 (Fig. 2C). To gain insight into the molecular basis for the differentiated profile of the FGF19 variant carrying the  $\beta$ 8– $\beta$ 9 loop mutation, we superimposed the crystal structures of FGF19 (PDB 2P23) (21) and  $\beta$ Klotho (PDB 5VAQ) (22) onto the X-ray structure for the ternary FGF23-Klotho-FGF receptor 1 (FGFR1) complex (PDB 5W21) (23) (Fig. 2D). Strikingly, the  $\beta$ 8– $\beta$ 9 loop, a surface-exposed region in FGF19 (indicated as red spheres in Fig. 2E), makes direct contact with the highly conserved linker region between Ig-like domain 2 (D2) and D3 in FGFR1. In this complex, multiple hydrogen bonds are predicted to form between the Gly-130 and Asn-132 residues in the  $\beta$ 8– $\beta$ 9 loop of FGF19 and Arg-250 in

FGFR1 (Fig. 2F), an invariant arginine residue conserved among the FGFR1, FGFR2, FGFR3, and FGFR4 receptors (Supplementary Fig. 3C and D).

With an absence of electron density for the N-terminus of FGF19 in published crystal structures (PDB 2P23 and 1PWA) (21,24), this domain of FGF19 remains poorly characterized with respect to both structure and function. Moreover, a lack of homology between the N-terminus of FGF19 and FGF23 limited the utility of modeling this region to the FGF23-Klotho-FGFR1 ternary structure. As a means toward better understanding the role this region plays in mediating the biological activities of FGF19, we used a systematic mutational analysis to precisely dissect this domain and identify the key residues involved in mediating these functions. As shown in Fig. 2G and H, several FGF19 mutants entirely lack the tumorigenic potential of wild-type FGF19, even while maintaining robust glucose-lowering activity in *db/db* mice. Relative to wild-type FGF19, liver weights were also reduced by these nontumorigenic mutants (Fig. 2I). On the basis of these fine-mapping analyses, amino acids 30–33 appear to be essential for both the metabolic and the proliferative activities of FGF19. A close inspection of the FGF23-FGFR (Fig. 2J and K and Supplementary Fig. 3E and F) and the FGF8-FGFR (Fig. 2L and Supplementary Fig. 3G) structures revealed that residues located in similar N-terminal positions make close contacts with the receptor. Therefore, changes in amino acids 30–33 in FGF19 may directly affect interactions with the receptor and influence downstream signaling. Additional in vivo SAR analyses are included in Supplementary Figs. 4 and 5. In summary, through an extensive SAR analysis, we identified distinct regions in FGF19 that are essential for its metabolic and proliferative features.

### A Randomized, Double-Blind, Placebo-Controlled Trial of an FGF19 Analog, NGM282, in Patients With Type 2 Diabetes

The identification of nontumorigenic FGF19 analogs with robust antidiabetic efficacy has ignited renewed interest in exploiting this class of hormones for therapeutic purpose. However, it has remained unproven whether these results from animal models represent a relevant glucose-lowering mechanism in humans. To functionally validate these findings

---

N-terminal region. Ten- to 12-week-old *db/db* mice were injected intravenously with  $3 \times 10^{11}$  vector genome AAV carrying FGF19, FGF19 mutants, or a control gene GFP. Glucose and body weight were measured before AAV injection (week 0) and at weeks 4 and 24 after AAV injection ( $n = 5$ – $6$  mice per group). H: Liver tumors in *db/db* mice expressing FGF19 mutants with deletions or mutations in the N-terminal region. The *db/db* mice were euthanized at the end of the study (24 weeks after AAV injection) for liver tumor quantification ( $n = 5$ – $6$  mice per group). I: Liver weight of *db/db* mice expressing FGF19 mutants with deletions or mutations in the N-terminal region ( $n = 5$ – $6$  mice per group). J: Alignment of amino acid sequences in the N-terminal regions. Note that the N-terminus of FGF19 shares no homology with FGF23, FGF8, or FGF2. The first  $\beta$ -sheet is shaded in blue. K: The N-terminus (N-ter) of FGF23 in the FGF23-Klotho-FGFR1 ternary complex (PDB 5W21). Note that the N-terminus of FGF23 directly interacts with the D3 domain of FGFR. L: The N-terminus of FGF8 in the FGF8-FGFR2 receptor complex (PDB 2FD8). Note that the N-terminus of FGF8 directly interacts with the D3 domain of FGFR. Data are mean  $\pm$  SEM. For glucose levels (A and G), we used two-way ANOVA with Sidak multiple comparison tests versus GFP; for liver tumors (B and H), we used one-way ANOVA with Dunnett multiple comparison tests versus FGF19. \* $P < 0.05$ , \*\* $P < 0.01$ , \*\*\* $P < 0.001$ .

---

in humans, we conducted a multicenter, randomized, double-blind, placebo-controlled study of the FGF19 variant NGM282 (N1–15 in Fig. 2G–I, also known as M70 [25]) in patients with type 2 diabetes.

A total of 81 patients were randomly assigned to receive daily doses of either NGM282 2 mg ( $n = 21$ ), NGM282 5 mg ( $n = 20$ ), NGM282 10 mg ( $n = 20$ ), or placebo ( $n = 20$ ) (Fig. 3). The patient characteristics of the study population are summarized in Table 1. NGM282 was administered subcutaneously daily for 28 consecutive days. After randomization but before NGM282 dosing, one patient in the NGM282 5-mg dose group withdrew from the study and was excluded from the analysis.

In contrast to results obtained from animal models, administration of NGM282 at any of the tested dose levels failed to relieve hyperglycemia in patients with type 2 diabetes as evidenced by the lack of significant change in plasma glucose or HbA<sub>1c</sub> levels (Fig. 4A–C). Improvements in insulin resistance on the basis of HOMA-IR were observed in patient cohorts treated with NGM282 5 and 10 mg, with a significant decrease at day 28 in participants treated with NGM282 10 mg ( $P < 0.001$  vs. baseline) (Fig. 4D). Levels of fasting insulin and HOMA- $\beta$ , a surrogate measure of insulin secretion, were decreased from baseline in the NGM282 10-mg group (Fig.

4E and F). Mean body weight and fructosamine levels decreased in patients treated with NGM282 10 mg versus those administered placebo (Table 2). No significant changes in oral GGTs were observed in any of the cohorts (Table 2).

Of note, serum levels of liver enzymes and those of ALT, and AST in particular, were significantly decreased in all NGM282 treatment groups as early as day 7 and remained lowered at day 28 (Fig. 4G). Elevated ALT ( $>40$  units/L) in patients with type 2 diabetes is highly predictive for NASH, a progressive form of nonalcoholic fatty liver disease (NAFLD) with risk of cirrhosis and liver failure (26). A dose-dependent decrease in ALT was observed with NGM282 in patients with presumptive NASH (ALT  $>40$  units/L at baseline) (Fig. 4H). No changes in alkaline phosphatase or  $\gamma$ -glutamyl transpeptidase were observed in NGM282-treated patients.

Given that FGF19 has been shown to control bile acid metabolism through actions on CYP7A1 (11), the first and rate-limiting enzyme in the classic pathway of bile acid synthesis, we conducted an exploratory analysis of serum levels of C4, a biomarker of hepatic CYP7A1 activity, in patients treated with the 2- and 5-mg doses of NGM282. Serum C4 concentrations were suppressed by 70% and 91% in patients treated with NGM282 2 mg and 5 mg, respectively, indicative of profound target engagement (Fig. 4I).

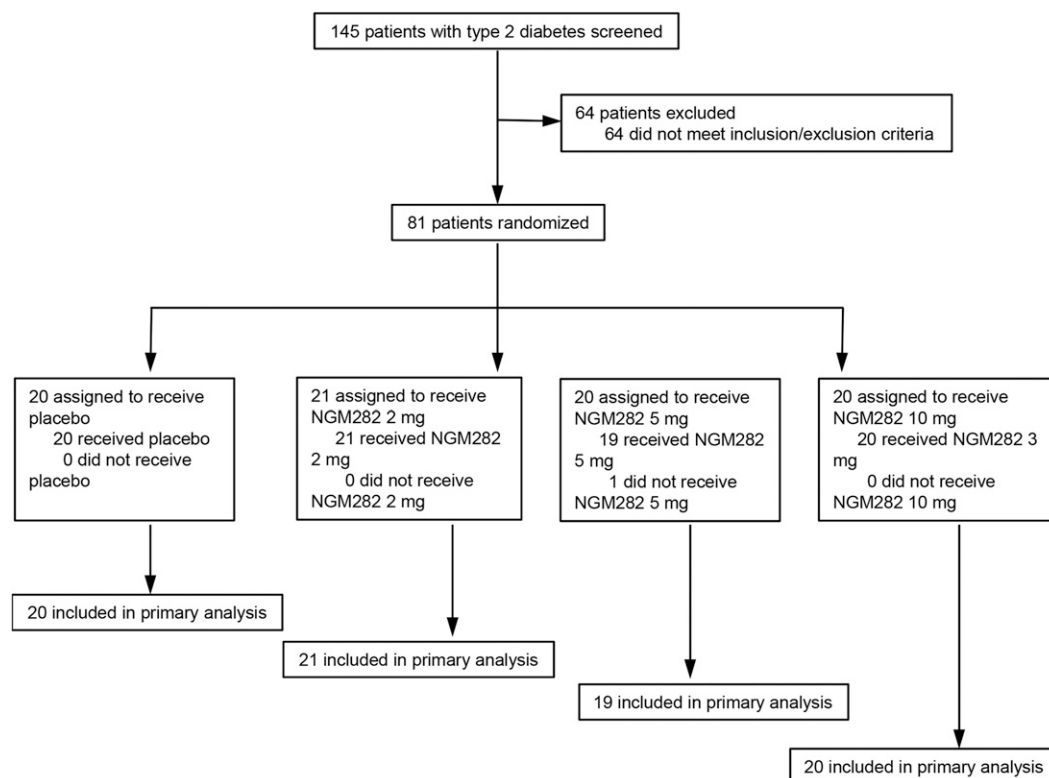


**Figure 3**—CONSORT flowchart. In this multicenter, randomized, double-blind, placebo-controlled study in patients with type 2 diabetes, 81 patients were randomized to receive either the FGF19 analog NGM282 at doses of 2 mg ( $n = 21$ ), 5 mg ( $n = 20$ ), or 10 mg ( $n = 20$ ) or placebo ( $n = 20$ ). One participant in the NGM282 5-mg dose group was withdrawn from the study after randomization but before NGM282 dosing for taking prednisone and was excluded from the analysis.

**Table 1—Baseline characteristics of patients with type 2 diabetes in a randomized, double-blind, placebo-controlled trial of NGM282**

	Placebo (n = 20)	NGM282 2 mg (n = 21)	NGM282 5 mg (n = 20)	NGM282 10 mg (n = 20)
Age (years)	57.3 ± 9.4	59.5 ± 6.9	55.9 ± 9.0	61.1 ± 8.4
Sex				
Male	15 (75)	15 (71)	12 (60)	16 (80)
Female	5 (25)	6 (29)	8 (40)	4 (20)
Race				
Asian	0	1 (5)	1 (5)	0
Black	0	0	0	0
White	14 (70)	17 (81)	17 (85)	15 (75)
Pacific Islander	0	0	0	1 (5)
Other	6 (30)	3 (14)	2 (10)	4 (20)
Metabolic factors				
Glucose (mg/dL)	169.2 ± 48.6	163.8 ± 27.0	158.4 ± 23.4	153.0 ± 34.2
HbA <sub>1c</sub> (%)	7.7 ± 0.7	7.5 ± 0.7	7.2 ± 0.4	7.2 ± 0.6
HbA <sub>1c</sub> (mmol/mol)	83.9 ± 7.6	81.8 ± 7.6	78.5 ± 4.4	78.5 ± 6.5
Fructosamine (μmol/L)	288.4 ± 47.8	277.2 ± 40.0	266.8 ± 35.9	269.7 ± 32.8
GTT glucose AUC	16.0 ± 3.2	15.9 ± 2.4	15.6 ± 2.2	15.5 ± 2.3
GTT insulin AUC	39.5 ± 30.7	37.9 ± 6.2	53.9 ± 29.3	50.2 ± 30.5
Insulin (μIU/mL)	13.9 ± 8.2	15.4 ± 6.0	18.9 ± 7.5	17.0 ± 9.2
HOMA-IR	4.8 ± 3.1	6.2 ± 2.5	7.5 ± 3.9	6.8 ± 5.0
HOMA-bcf	58.1 ± 58.0	56.5 ± 26.5	67.4 ± 26.4	75.4 ± 67.4
Weight (kg)	97.6 ± 18.6	95.3 ± 15.5	95.5 ± 14.7	95.7 ± 16.0
BMI (kg/m <sup>2</sup> )	32.4 ± 4.8	32.0 ± 4.5	32.2 ± 3.5	32.1 ± 4.6
Liver enzymes (units/L)				
ALP	75.0 ± 34.3	65.3 ± 23.4	65.7 ± 16.6	77.9 ± 30.6
ALT	33.9 ± 16.7	27.6 ± 10.6	36.7 ± 25.9	34.4 ± 19.8
AST	25.1 ± 11.4	21.5 ± 7.6	27.4 ± 14.9	26.4 ± 11.5
GGT	60.6 ± 104.9	32.5 ± 17.3	35.4 ± 13.9	53.0 ± 36.6

Data are n (%) or mean ± SD. AUC, area under curve; GGT, γ-glutamyl transpeptidase.

Overall, NGM282 appears to be well tolerated in patients with type 2 diabetes. Although 68 (85%) of the 80 patients experienced at least one AE, the majority of AEs were limited to grade 1 events (78%,  $n = 62$ ). The most commonly reported AEs (>10%) were diarrhea (32%,  $n = 26$ ), nausea (32%,  $n = 26$ ), injection site bruising (18%,  $n = 14$ ), injection site pruritus (16%,  $n = 13$ ), and headache (15%,  $n = 12$ ) (Supplementary Table 6). These AEs were reported more frequently in the NGM282 groups than in the placebo group. Nine participants withdrew from the study early mostly because of gastrointestinal symptoms (two in the NGM282 2-mg group, three in the 5-mg group, three in the 10-mg group, and one in the placebo group). No serious AEs, life-threatening events (grade 4), or patient deaths (grade 5) were reported in any treatment group during the course of the study.

In summary, administration of NGM282 for 28 days in patients with type 2 diabetes did not produce a significant glucose-lowering effect. However, the observed reductions in ALT, AST, and HOMA-IR and marked suppression of C4 are indicative of potent target engagement.

#### FGF19 and NGM282 Ameliorates Liver Inflammation and Fibrosis Associated With NASH

The lack of glucose-lowering activity of NGM282 in patients with type 2 diabetes suggests that FGF19 signaling

may not be responsible for the rapid diabetes remission after gastric bypass surgery in humans. However, gastric bypass surgery's clinical benefits are not limited to diabetes remission, but include correction of a wide range of metabolic dysfunctions, including NASH (27–29). The observation that C4, ALT, and AST (key parameters relevant to the pathogenesis of NASH) decreased with NGM282 treatment spurred interest in evaluating the FGF19 pathway in patients with NASH.

Strikingly, hepatic CYP7A1 expression was significantly elevated in patients with NASH compared with healthy subjects in multiple microarray data sets (Fig. 5A). Of note, lower FGF19 levels, as well as elevated hepatic βKlotho and FGFR4 expression, were observed in patients with NASH, suggesting that the FGF19-βKlotho-FGFR4 pathway may be modulated in a clinically and physiologically relevant manner in this population (Fig. 5B).

We examined the effect of FGF19 and NGM282 on disease progression, and liver fibrosis in particular, in a mouse model of severe NASH (Fig. 5C). Treatment of HFFCD-fed, *Fxr*-deficient mice with FGF19 or NGM282 significantly improved serum levels of ALT and AST and reduced circulating concentrations of TBAs (Fig. 5D). Hepatic mRNA levels of bile acid synthetic enzymes, markers of monocyte/macrophage infiltration, markers of stellate cell/myofibroblast activation, and

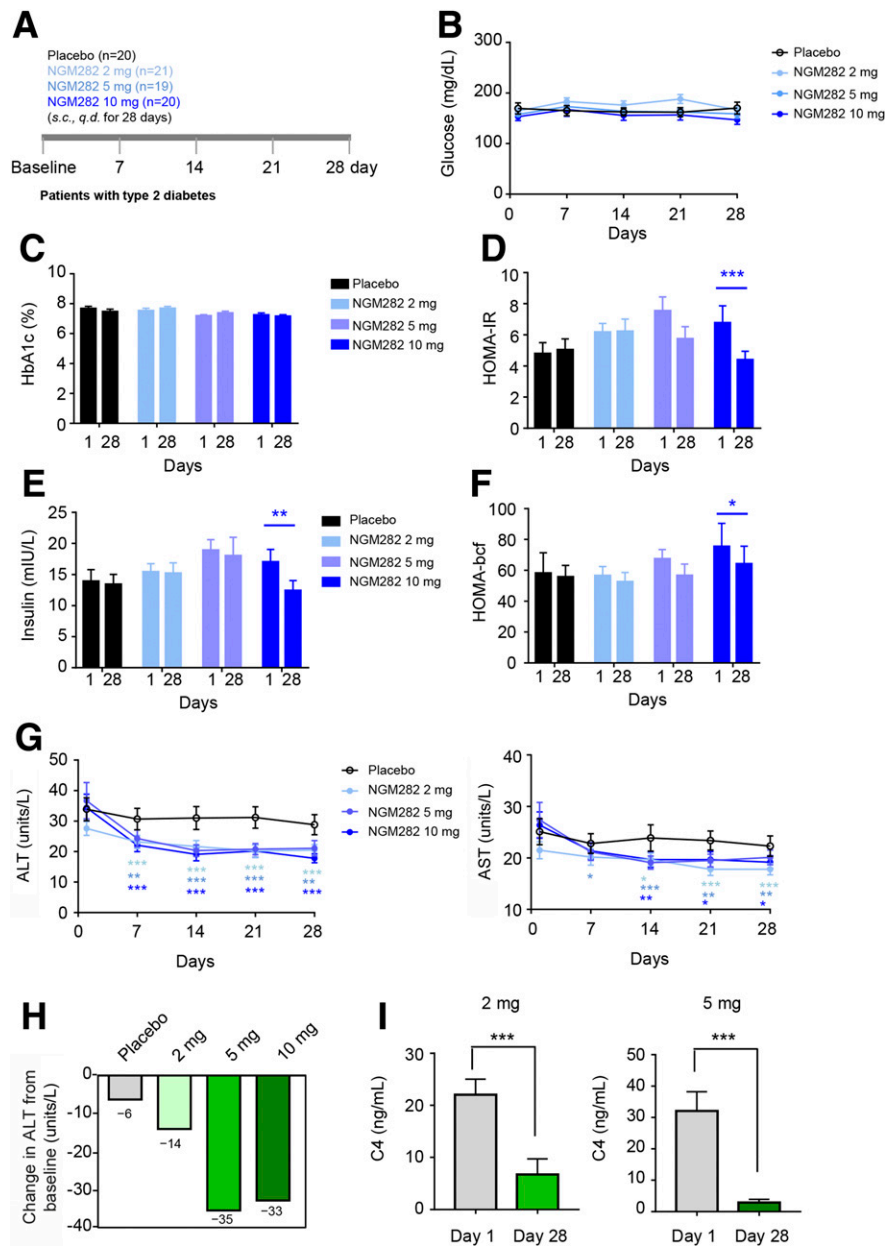


**Figure 4**—A randomized, double-blind, placebo-controlled trial of the FGF19 analog NGM282 in patients with type 2 diabetes. **A**: Trial design. NGM282 was administered daily for 28 consecutive days. **B**: Fasting blood glucose over time. **C**: HbA<sub>1c</sub> levels at baseline (predose on day 1) and day 28. **D**: HOMA-IR at baseline and day 28. **E**: Fasting insulin concentrations at baseline and day 28. **F**: HOMA-bcf at baseline and day 28. **G**: Levels of ALT and AST over time. **H**: Change in ALT from baseline to day 28 in patients with presumptive NASH (ALT >40 units/L at baseline). **I**: Serum concentrations of C4 at baseline and day 28 in patients treated with NGM282 2 mg or 5 mg. Data are mean ± SEM. \**P* < 0.05, \*\**P* < 0.01, \*\*\**P* < 0.001 by paired two-tailed *t* test. q.d., daily; s.c., subcutaneous.

fibrosis were notably decreased by FGF19 or NGM282 treatment (Fig. 5E–H). Morphometric quantification of Sirius red-stained collagen area revealed evidently less fibrosis in FGF19- or NGM282-treated animals (Fig. 5I and J). Mice administered FGF19 and NGM282 had lower circulating insulin, suggestive of improved insulin resistance (Fig. 5K). Overall, FGF19 and NGM282 demonstrated anti-inflammatory and antifibrotic activities in a mouse model of NASH in an *Fxr*-independent manner.

On the basis of the results described above, as well as studies in HFFCD-fed C57BL/6 mice (30), we conducted a multicenter, randomized, double-blind, placebo-controlled study to assess effects of NGM282 in patients with biopsy-confirmed NASH. As we reported recently (12), a 12-week treatment with NGM282 produced rapid and significant reductions in liver fat content, ALT, AST, and biomarkers of fibrosis in patients with NASH. Importantly, treatment with NGM282 improved NASH-related

**Table 2—Change in key outcome measures from baseline to day 28 in a randomized, double-blind, placebo-controlled trial of NGM282 in patients with type 2 diabetes**

Key outcome measure	Difference in least squares means (95% CI) (NGM282 vs. placebo)					
	NGM282 2 mg (n = 21)	P value	NGM282 5 mg (n = 19)	P value	NGM282 10 mg (n = 20)	P value
Glucose (mg/dL)	0 (−12.6, 12.6)	1.00	−7.2 (−19.8, 9.0)	0.94	−7.2 (−19.8, 9.0)	0.94
HbA <sub>1c</sub> (%)	0.25 (0, 0.5)	0.19	0.3 (0, 0.5)	0.19	0 (−0.3, 0.4)	0.76
HbA <sub>1c</sub> (mmol/mol)	2.7 (0, 5.5)	0.19	3.3 (0, 5.5)	0.19	0 (−3.3, 4.4)	0.76
Fructosamine (μmol/L)	2.6 (−14.3, 19.4)	0.97	−1.7 (−19.3, 15.9)	0.99	−17.7 (−35.0, −0.5)	0.043
GTT glucose AUC	0.8 (−1.1, 2.6)	0.66	1.0 (−1.0, 3.1)	0.46	0.5 (−1.5, 2.5)	0.89
GTT insulin AUC	−6.0 (−12.2, 0.8)	0.22	−8.3 (−16.7, −2.8)	0.06	−7.4 (−21.0, 0.8)	0.22
Insulin (μIU/mL)	−1.5 (−6.7, 3.6)	0.80	−1.0 (−6.9, 4.8)	0.95	−3.7 (−9.5, 2.0)	0.28
HOMA-IR	0.9 (−1.3, 3.1)	0.60	0.9 (−1.5, 3.4)	0.66	−0.9 (−3.2, 1.4)	0.64
HOMA-bcf	−4.5 (−16.0, 11.0)	1.00	−1.5 (−19.0, 17.0)	1.00	−13.5 (−27.0, 6.0)	0.30
Weight (kg)	−0.6 (−1.9, 0.6)	0.50	−0.7 (−2.0, 0.6)	0.46	−1.5 (−2.8, −0.2)	0.019

SAS 9.4 was used for all analyses. The difference between NGM282 and placebo groups was analyzed using ANCOVA, with treatment group as a factor and baseline values of the outcome as covariates. All statistical analyses were carried out using two-sided tests at the 5% level of significance. AUC, area under curve.

histology, including NAFLD activity score and fibrosis stage, in 12 weeks in patients with NASH (31). Thus, NGM282 demonstrated remarkable efficacy in improving the histological and biochemical features of NASH, mimicking the beneficial effect of bariatric surgery on alleviating NASH.

## DISCUSSION

Although bariatric surgery was initially considered a surgical procedure to promote nutrient malabsorption, a growing body of evidence indicates that restriction and malabsorption are not the primary mechanisms driving the metabolic improvements associated with bariatric surgery. We identify FGF19 as a gut hormone that is rapidly (i.e., within 7 days) induced by bariatric surgery and, moreover, demonstrate that pharmacological administration of FGF19 or its analog NGM282 mimics many of the beneficial metabolic effects of this procedure in animal models and humans. These findings have important implications for therapies aimed at simulating bariatric surgery in humans.

Although bile acids and FXR signaling are implicated as the molecular underpinnings for the beneficial effects of bariatric surgery (32,33), and the elevated FGF19 concentrations were observed in patients who underwent the surgery (34–37), most of these studies examined FGF19 levels in small numbers of patients or at time points too late to implicate a causative role of hormonal change in the metabolic effects. Our study is the first report to our knowledge that has convincingly shown that FGF19 levels are elevated as early as 7 days postsurgery in humans, addressing an important knowledge gap in understanding the mechanisms for metabolic improvements observed shortly after bariatric surgery.

Despite the impressive metabolic efficacy demonstrated in preclinical models, as shown in this report and previously

(38,39), safety and ethical concerns have prevented researchers from testing FGF19 in the clinic, since mice expressing an FGF19 transgene develop hepatocellular carcinomas (16). To address these concerns, we used an unbiased, systematic, in vivo screen to engineer and characterize FGF19 analogs that lack tumorigenic potential and thereby enable the first-in-human testing of an FGF19-based therapy. As shown in the current study, FGF19 dramatically improves glycemic control in multiple rodent models of diabetes of differing etiology, recapitulating the rapid, weight loss-independent impact on glycemic control after gastric bypass surgery in patients with diabetes. The antidiabetic effect of FGF19 in these models is likely mediated by the FGFR1c-βKlotho receptor complex through its action on the nervous system (40). These results are also consistent with previous studies demonstrating that FGF19 increases metabolic rate and reduces adiposity in mice (38), acts as a postprandial, insulin-independent activator of hepatic glycogen and protein synthesis (11), regulates hepatic glucose metabolism by inhibiting the CREB-peroxisome proliferator-activated receptor γ coactivator-1α pathway (11), and improves glucose effectiveness through the hypothalamus-pituitary-adrenal axis (41,42). Given that FGF19 can stimulate adiponectin expression and production by adipose tissue (43) and that circulating adiponectin levels are increased after RYGB (44), it is possible that one of the mechanisms by which FGF19 and NGM282 improve NAFLD and NASH is the induction of adiponectin. Indeed, we have recently reported that selective activation of the FGFR1-βKlotho complex with an agonistic antibody increased serum adiponectin, and a high-molecular-weight form of adiponectin in particular, in obese patients (45).

Contrary to expectations from the field, we report here that the FGF19 analog NGM282 lacks the glucose-lowering activity so compellingly demonstrated in animal models

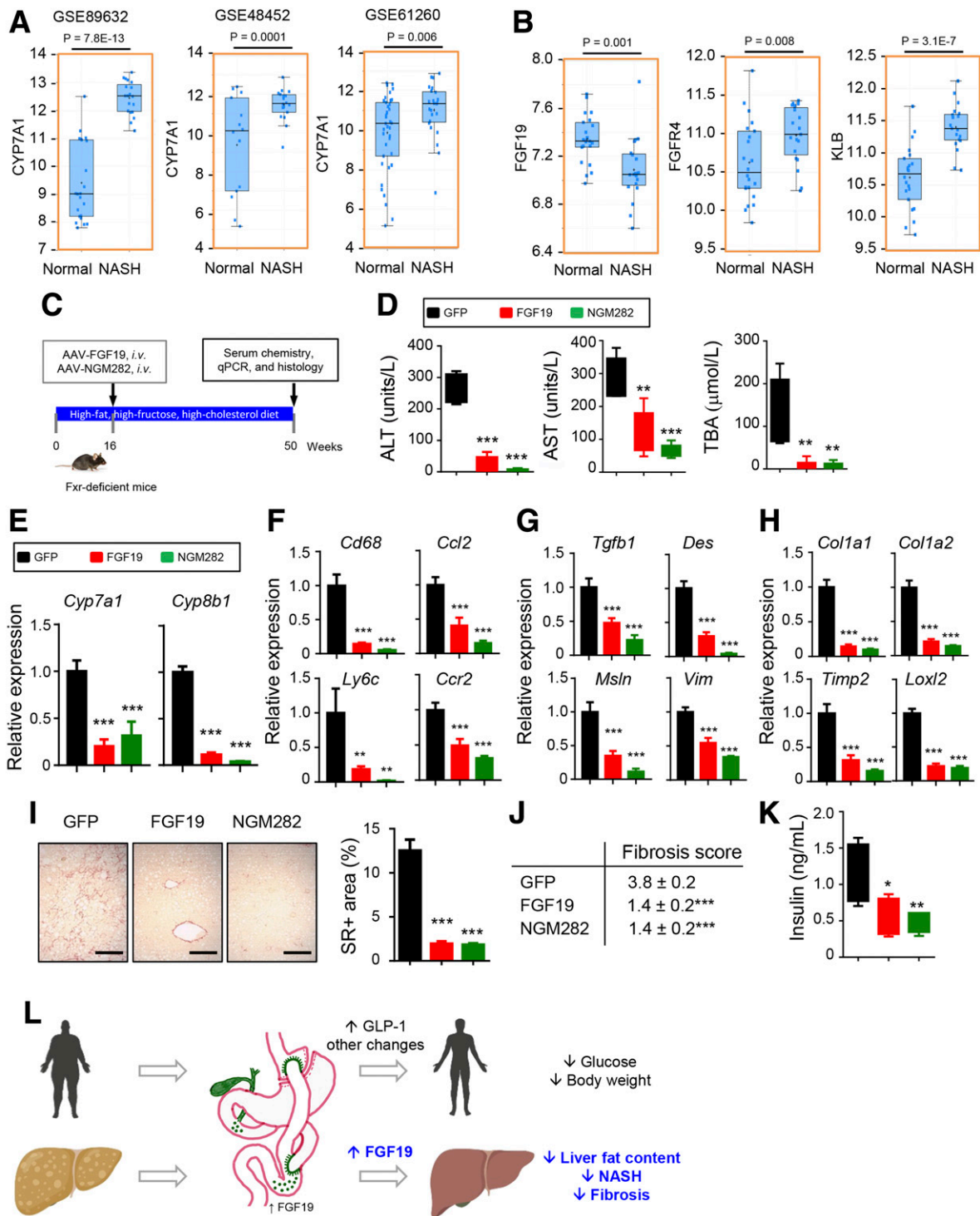


**Figure 5**—FGF19 and NGM282 ameliorates liver inflammation and fibrosis associated with NASH. **A**: Hepatic CYP7A1 mRNA levels are elevated in patients with NASH compared with normal subjects. Results from three independent cohorts (Gene Expression Omnibus data sets GSE89632, GSE48452, and GSE61260) are shown. **B**: Expression of FGF19 is lower, whereas expression of receptors FGFR4 and βKlotho (KLB) is higher, in patients with NASH compared with normal subjects. Shown are data from GSE89632. **C**: Study design. *Fxr*-deficient mice were fed an HFFCD to induce NASH. Treatment was initiated after 16 weeks of HFFCD feeding by intravenously (i.v.) injecting mice with AAV-FGF19, AAV-NGM282, or a control virus AAV-GFP through tail veins. HFFCD feeding was continued for an additional 34 weeks when mice were euthanized for gene expression and histology analysis. **D**: FGF19 and NGM282 reduce serum concentrations of ALT, AST, and TBAs (*n* = 5 mice per group). **E**: FGF19 and NGM282 suppress hepatic expression of *Cyp7a1* and *Cyp8b1* by quantitative PCR (qPCR) analysis (*n* = 10 biologically independent samples per group). **F**: FGF19 and NGM282 inhibit expression of proinflammatory genes (*n* = 10 biologically independent samples per group). **G**: FGF19 and NGM282 inhibit expression of markers of stellate cell activation (*n* = 10 biologically independent samples per group). **H**: FGF19 and NGM282 reduce expression of fibrosis-related genes (*n* = 10 biologically independent samples per group). **I**: Representative images of livers stained with Sirius red. Sirius red stains collagen red, indicative of liver

when tested in patients with type 2 diabetes. However, NGM282 proved highly effective in patients with NASH, significantly reducing liver fat content (12) and NASH-related histological features (31). The scale of the effect of NGM282 and the ability to elicit robust response in nearly 90% of patients indicate that FGF19 may be a key driver of improvements in fatty liver and NASH by gastric bypass surgery. Furthermore, NGM282 achieved reductions in liver fat content more rapidly (−60% in liver fat content after 12-week treatment) than RYGB (−73% in liver fat content 1 year after surgery) (28) or FXR agonist obeticholic acid (−17% in liver fat content after 72-week treatment) (46). We hypothesize that endogenously mounted FGF19 induction by either RYGB or FXR agonists requires a longer time to inhibit NASH progression but that a pharmacological intervention could achieve greater exposure and a faster, more robust effect. Although NASH is considered a manifestation of metabolic syndrome in the liver, whether NASH is a cause or a consequence of type 2 diabetes has long been the subject of debate. The pronounced anti-NASH activity without associated antihyperglycemic activity of NGM282 is consistent with genetic studies suggesting that excess hepatic fat is associated with progressive liver disease but does not always increase the risk of type 2 diabetes. Perhaps the deficit in  $\beta$ -cell/islet function is a predominant underlying factor in hyperglycemia that is not corrected by lowering intrahepatic fat and inflammation. The current trial reminds us of the need for a careful reexamination of previous conclusions drawn from animal studies regarding a role for FGF19 in glucose regulation and that the clinical development of FGF19 analogs should focus instead on liver diseases.

The discovery of NGM282 through an *in vivo* SAR screen represents the culmination of years of careful work that yielded the first FGF19 analog for testing in humans. Large-scale *in vitro* biochemical or cell-based screens with sufficient throughput have been routinely used to identify new compounds. However, maintaining relevance to complex disease pathophysiology is challenging. No single *in vitro* assay can predict outcomes in systemic diseases that involve multiple organs, such as diabetes and cancer. Advances in gene delivery using AAV enabled us to efficiently evaluate a large number of engineered FGF19 molecules for prolonged periods of time in mice. The results of our efforts to apply an *in vivo* approach as a means of investigating the metabolic and

cancer dependencies of FGF19 demonstrate the feasibility of systematically dissecting a complex SAR in great detail, representing new avenues for the development of potential therapeutics. Results from our *in vivo* SAR analysis and structural modeling revealed novel mechanistic insights consistent with a model that the N-terminus of FGF19 is intrinsically disordered when unbound but, upon binding to FGFR, makes close contact with the D3 domain of FGFR. Changes in amino acid sequence in the N-terminal region may result in conformational shifts in the ternary FGF19- $\beta$ Klotho-FGFR complex that lead to diverse downstream signaling. This may explain why, unlike wild-type FGF19, NGM282 does not activate STAT3, a signaling pathway essential for FGF19-mediated hepatocarcinogenesis. Moreover, we identified a novel region ( $\beta$ 8– $\beta$ 9 loop) in FGF19 that is crucial for both glucoregulatory and tumorigenic activities.

The underlying molecular mechanism contributing to the benefits of bariatric surgery remains an area of active investigation. Several potential mechanisms have been proposed, including an increased secretion of gut hormone GLP-1 (47). Given the well-established glucose-lowering effect of GLP-1 analogs in humans, GLP-1 could be the surgical factor for diabetes remission. However, GLP-1 analogs have failed to demonstrate a robust reduction in liver fat content to levels that are seen in patients who had undergone gastric bypass (48,49). In contrast, although its effect on the regulation of glucose hemostasis may be limited in humans, FGF19 analog can rapidly and markedly reduce liver fat content and improve NASH-related histology. Together, FGF19 and GLP-1 may be the long-sought-after surgical factors that contribute to the improvement in fatty liver, NASH, and diabetes by gastric bypass surgery (Fig. 5L). Loss-of-function studies, such as those requiring the use of mice deficient in FGF15 (the murine ortholog of FGF19), are needed but challenging because of species-specific divergent regulation of metabolism and carcinogenesis by FGF19 and FGF15 (50). Unlike FGF19, FGF15 does not exert glucose-lowering, HbA<sub>1c</sub>-normalizing effects in diabetic animals. A further complication arises from the fact that FGF15-deficient mice are healthy only when bred on a mixed background, and crossing to the C57BL/6 strain, the gold standard in mouse genetic studies, resulted in progressive loss of homozygous mice. These difficulties pose substantial challenges for the accurate and timely characterization of loss of function in animal models.

---

fibrosis. Morphometric quantifications of Sirius red-positive (SR+) area as percentage of total liver area are also shown. Scale bars = 100  $\mu$ m. *J*: Fibrosis scores using Kleiner criteria ( $n = 5$  mice per group). *K*: Serum concentrations of insulin ( $n = 5$  mice per group). *L*: Reprogramming of intestinal architecture through gastric bypass surgery increases circulating levels of two gut hormones, FGF19 and GLP-1. GLP-1 analogs, however, have previously failed to demonstrate a robust reduction in liver fat content to levels that are seen in patients who have undergone gastric bypass, despite its well-established role in glycemic control. Although the effects of FGF19 analog on the regulation of glucose hemostasis may be limited in humans, it can rapidly and markedly reduce liver fat content and improve NASH-related histology. Together, FGF19 and GLP-1 may be the long-sought-after surgical factors that contribute to the improvement in fatty liver, NASH, and diabetes by gastric bypass surgery. Data are mean  $\pm$  SEM. \* $P < 0.05$ , \*\* $P < 0.01$ , \*\*\* $P < 0.001$  versus GFP by one-way ANOVA with Dunnett multiple comparison tests.

---

In summary, our results demonstrated that the gut hormone FGF19 likely plays a direct role in the metabolic improvements observed after gastric bypass surgery, although its effects on the regulation of glucose homeostasis may be limited in humans. The translation of preclinical findings is an inherently unpredictable and time-consuming process; great care must be exercised before testing new drugs in humans. NGM282 has cleared rigorous safety testing in multiple preclinical species, including nonhuman primate models. As clinical data are accumulating, it is emerging that the regulation of metabolism by the FGF19 pathway may be more complex than initially assumed. The present work has important clinical implications and advances our understanding of the biological processes that underlie bariatric surgery. Exploitation of the FGF19 signaling pathway by informed engineering of selective modulators of the FGFRs could represent a pharmacological approach to replacing the bariatric procedure with equally effective but less invasive treatments.

**Acknowledgments.** The authors thank all the patients who participated in the clinical studies and the investigators, study coordinators, and staff of all of the participating clinical centers for support and assistance. The authors thank Dr. Jin-Long Chen and Dr. Darrin Lindhout (NGM Biopharmaceuticals) for advice and insightful discussions. The authors also thank Hong Yang, Mark Humphrey, Van Phung, Josh Lichtman, Yi Fritz, Yarong Lu, and Andrew Yan (NGM Biopharmaceuticals) for technical assistance and NGM Biopharmaceuticals Vivarium staff for the care of the animals used in the studies.

**Duality of Interest.** This study was funded by NGM Biopharmaceuticals. A.M.D., M.Z., D.D.K., R.M.L., H.T., and L.L. report being employees and stockholders of NGM Biopharmaceuticals. No other potential conflicts of interest relevant to this article were reported.

**Author Contributions.** A.M.D., M.Z., D.D.K., S.C.H., T.D.A., R.M.L., H.T., and L.L. contributed to the study design and writing of the manuscript. A.M.D., M.Z., D.D.K., S.C.H., T.D.A., and L.L. contributed to the study investigation and data collection. A.M.D., H.T., and L.L. contributed to the study conceptualization. L.L. is the guarantor of this work and, as such, had full access to all the data in the study and takes responsibility for the integrity of the data and the accuracy of the data analysis.

**Data Availability.** The data sets generated and/or analyzed during the current study are available in public repositories (<http://www.ncbi.nlm.nih.gov/gds> for the Gene Expression Omnibus database and <https://www.rcsb.org> for the Protein Data Bank database). Graphic artwork was created using BioRender software. The resource generated during the current study is available from the corresponding author upon reasonable request under a material transfer agreement.

## References

- Danaei G, Finucane MM, Lu Y, et al.; Global Burden of Metabolic Risk Factors of Chronic Diseases Collaborating Group (Blood Glucose). National, regional, and global trends in fasting plasma glucose and diabetes prevalence since 1980: systematic analysis of health examination surveys and epidemiological studies with 370 country-years and 2.7 million participants. *Lancet* 2011;378:31–40
- GBD 2016 Causes of Death Collaborators. Global, regional, and national age-sex specific mortality for 264 causes of death, 1980–2016: a systematic analysis for the Global Burden of Disease Study 2016. *Lancet* 2017;390:1151–1210
- Adams TD, Davidson LE, Litwin SE, et al. Weight and metabolic outcomes 12 years after gastric bypass. *N Engl J Med* 2017;377:1143–1155
- Mingrone G, Panunzi S, De Gaetano A, et al. Bariatric surgery versus conventional medical therapy for type 2 diabetes. *N Engl J Med* 2012;366:1577–1585
- Schauer PR, Kashyap SR, Wolski K, et al. Bariatric surgery versus intensive medical therapy in obese patients with diabetes. *N Engl J Med* 2012;366:1567–1576
- Rubino F, Gagner M, Gentileschi P, et al. The early effect of the Roux-en-Y gastric bypass on hormones involved in body weight regulation and glucose metabolism. *Ann Surg* 2004;240:236–242
- Patti ME, Houten SM, Bianco AC, et al. Serum bile acids are higher in humans with prior gastric bypass: potential contribution to improved glucose and lipid metabolism. *Obesity (Silver Spring)* 2009;17:1671–1677
- Jiao J, Bae EJ, Bandyopadhyay G, et al. Restoration of euglycemia after duodenal bypass surgery is reliant on central and peripheral inputs in Zucker fa/fa rats. *Diabetes* 2013;62:1074–1083
- Myronovych A, Kirby M, Ryan KK, et al. Vertical sleeve gastrectomy reduces hepatic steatosis while increasing serum bile acids in a weight-loss-independent manner. *Obesity (Silver Spring)* 2014;22:390–400
- Kohli R, Setchell KD, Kirby M, et al. A surgical model in male obese rats uncovers protective effects of bile acids post-bariatric surgery. *Endocrinology* 2013;154:2341–2351
- Kliwer SA, Mangelsdorf DJ. Bile acids as hormones: the FXR-FGF15/19 pathway. *Dig Dis* 2015;33:327–331
- Harrison SA, Rinella ME, Abdelmalek MF, et al. NGM282 for treatment of non-alcoholic steatohepatitis: a multicentre, randomised, double-blind, placebo-controlled, phase 2 trial. *Lancet* 2018;391:1174–1185
- Hirschfield GM, Chazouilleres O, Drenth JP, et al. Effect of NGM282, an FGF19 analogue, in primary sclerosing cholangitis: a multicenter, randomized, double-blind, placebo-controlled phase II trial. *J Hepatol* 2019;70:483–493
- Mayo MJ, Wigg AJ, Leggett BA, et al. NGM282 for treatment of patients with primary biliary cholangitis: a multicenter, randomized, double-blind, placebo-controlled trial. *Hepatol Commun* 2018;2:1037–1050
- Rubino F, Marescaux J. Effect of duodenal-jejunal exclusion in a non-obese animal model of type 2 diabetes: a new perspective for an old disease. *Ann Surg* 2004;239:1–11
- Nicholes K, Guillet S, Tomlinson E, et al. A mouse model of hepatocellular carcinoma: ectopic expression of fibroblast growth factor 19 in skeletal muscle of transgenic mice. *Am J Pathol* 2002;160:2295–2307
- Wu X, Ge H, Lemon B, et al. Separating mitogenic and metabolic activities of fibroblast growth factor 19 (FGF19). *Proc Natl Acad Sci U S A* 2010;107:14158–14163
- Goetz R, Ohnishi M, Kir S, et al. Conversion of a paracrine fibroblast growth factor into an endocrine fibroblast growth factor. *J Biol Chem* 2012;287:29134–29146
- Suh JM, Jonker JW, Ahmadian M, et al. Endocrinization of FGF1 produces a neomorphic and potent insulin sensitizer. *Nature* 2014;513:436–439
- Wu AL, Coulter S, Liddle C, et al. FGF19 regulates cell proliferation, glucose and bile acid metabolism via FGFR4-dependent and independent pathways. *PLoS One* 2011;6:e17868
- Goetz R, Beenken A, Ibrahim OA, et al. Molecular insights into the klotho-dependent, endocrine mode of action of fibroblast growth factor 19 subfamily members. *Mol Cell Biol* 2007;27:3417–3428
- Lee S, Choi J, Mohanty J, et al. Structures of  $\beta$ -klotho reveal a 'zip code'-like mechanism for endocrine FGF signalling. *Nature* 2018;553:501–505
- Chen G, Liu Y, Goetz R, et al.  $\alpha$ -Klotho is a non-enzymatic molecular scaffold for FGF23 hormone signalling. *Nature* 2018;553:461–466
- Harmer NJ, Pellegrini L, Chirgadze D, Fernandez-Recio J, Blundell TL. The crystal structure of fibroblast growth factor (FGF) 19 reveals novel features of the FGF family and offers a structural basis for its unusual receptor affinity. *Biochemistry* 2004;43:629–640
- Zhou M, Wang X, Phung V, et al. Separating tumorigenicity from bile acid regulatory activity for endocrine hormone FGF19. *Cancer Res* 2014;74:3306–3316
- Rinella ME. Nonalcoholic fatty liver disease: a systematic review. *JAMA* 2015;313:2263–2273
- Barker KB, Palekar NA, Bowers SP, Goldberg JE, Pulcini JP, Harrison SA. Non-alcoholic steatohepatitis: effect of Roux-en-Y gastric bypass surgery. *Am J Gastroenterol* 2006;101:368–373

28. Lassailly G, Caiazzo R, Buob D, et al. Bariatric surgery reduces features of nonalcoholic steatohepatitis in morbidly obese patients. *Gastroenterology* 2015; 149:379–388; quiz e15-16
29. Jirapinyo P, Thompson CC. Treatment of NASH with gastric bypass. *Curr Gastroenterol Rep* 2018;20:49
30. Zhou M, Learned RM, Rossi SJ, DePaoli AM, Tian H, Ling L. Engineered FGF19 eliminates bile acid toxicity and lipotoxicity leading to resolution of steatohepatitis and fibrosis in mice. *Hepatology* 2017;1:1024–1042
31. Harrison SA, Rossi SJ, Paredes AH, et al. NGM282 improves liver fibrosis and histology in 12 weeks in patients with nonalcoholic steatohepatitis. *J Hepatol* 25 February 2019 [Epub ahead of print]. DOI: 10.1002/hep.30590
32. Ryan KK, Tremaroli V, Clemmensen C, et al. FXR is a molecular target for the effects of vertical sleeve gastrectomy. *Nature* 2014;509:183–188
33. Bozadjieva N, Heppner KM, Seeley RJ. Targeting FXR and FGF19 to treat metabolic diseases—lessons learned from bariatric surgery. *Diabetes* 2018;67: 1720–1728
34. Jansen PL, van Werven J, Aarts E, et al. Alterations of hormonally active fibroblast growth factors after Roux-en-Y gastric bypass surgery. *Dig Dis* 2011;29:48–51
35. Pournaras DJ, Glicksman C, Vincent RP, et al. The role of bile after Roux-en-Y gastric bypass in promoting weight loss and improving glycaemic control. *Endocrinology* 2012;153:3613–3619
36. Gerhard GS, Styer AM, Wood GC, et al. A role for fibroblast growth factor 19 and bile acids in diabetes remission after Roux-en-Y gastric bypass. *Diabetes Care* 2013;36:1859–1864
37. Nemati R, Lu J, Dokpuang D, Booth M, Plank LD, Murphy R. Increased bile acids and FGF19 after sleeve gastrectomy and Roux-en-Y gastric bypass correlate with improvement in type 2 diabetes in a randomized trial. *Obes Surg* 2018;28: 2672–2686
38. Tomlinson E, Fu L, John L, et al. Transgenic mice expressing human fibroblast growth factor-19 display increased metabolic rate and decreased adiposity. *Endocrinology* 2002;143:1741–1747
39. Fu L, John LM, Adams SH, et al. Fibroblast growth factor 19 increases metabolic rate and reverses dietary and leptin-deficient diabetes. *Endocrinology* 2004;145:2594–2603
40. Lan T, Morgan DA, Rahmouni K, et al. FGF19, FGF21, and an FGFR1/ $\beta$ -Klotho-activating antibody act on the nervous system to regulate body weight and glycemia. *Cell Metab* 2017;26:709–718.e3
41. Morton GJ, Matsen ME, Bracy DP, et al. FGF19 action in the brain induces insulin-independent glucose lowering. *J Clin Invest* 2013;123:4799–4808
42. Perry RJ, Lee S, Ma L, Zhang D, Schlessinger J, Shulman GI. FGF1 and FGF19 reverse diabetes by suppression of the hypothalamic-pituitary-adrenal axis. *Nat Commun* 2015;6:6980
43. You M, Zhou Z, Daniels M, Jogasuria A. Endocrine adiponectin-FGF15/19 Axis in ethanol-induced inflammation and alcoholic liver injury. *Gene Expr* 2018; 18:103–113
44. Swarbrick MM, Stanhope KL, Austrheim-Smith IT, et al. Longitudinal changes in pancreatic and adipocyte hormones following Roux-en-Y gastric bypass surgery. *Diabetologia* 2008;51:1901–1911
45. DePaoli AM, Phung V, Yan AZ, Ling L, Baxter BA, Tian H: NGM313, a novel activator of  $\beta$ klotho/FGFR1c: single dose PK, safety and tolerability, coupled with an increase in adiponectin (a marker of target engagement and insulin sensitivity) support potential for treatment of NASH. Poster presented at NASH-TAG 19, 3–5 January 2019, at the Chateau Deer Valley, Park City, UT
46. Neuschwander-Tetri BA, Loomba R, Sanyal AJ, et al.; NASH Clinical Research Network. Farnesoid X nuclear receptor ligand obeticholic acid for non-cirrhotic, non-alcoholic steatohepatitis (FLINT): a multicentre, randomised, placebo-controlled trial. *Lancet* 2015;385:956–965
47. Thaler JP, Cummings DE. Minireview: hormonal and metabolic mechanisms of diabetes remission after gastrointestinal surgery. *Endocrinology* 2009;150: 2518–2525
48. Smits MM, Tonneijck L, Muskiet MH, et al. Twelve week liraglutide or sitagliptin does not affect hepatic fat in type 2 diabetes: a randomised placebo-controlled trial. *Diabetologia* 2016;59:2588–2593
49. Tang A, Rabasa-Lhoret R, Castel H, et al. Effects of insulin glargine and liraglutide therapy on liver fat as measured by magnetic resonance in patients with type 2 diabetes: a randomized trial. *Diabetes Care* 2015;38:1339–1346
50. Zhou M, Luo J, Chen M, et al. Mouse species-specific control of hepatocarcinogenesis and metabolism by FGF19/FGF15. *J Hepatol* 2017;66:1182–1192